AIP | Applied Physics Letters

Homoepitaxial growth of β-Ga2O3 thin films by low pressure chemical vapor deposition

Subrina Rafique, Lu Han, Marko J. Tadjer, Jaime A. Freitas Jr., Nadeemullah A. Mahadik, and Hongping Zhao

Citation: Applied Physics Letters **108**, 182105 (2016); doi: 10.1063/1.4948944
View online: http://dx.doi.org/10.1063/1.4948944
View Table of Contents: http://scitation.aip.org/content/aip/journal/apl/108/18?ver=pdfcov
Published by the AIP Publishing

Homoepitaxial growth of β-Ga_2O_3 thin films by low pressure chemical vapor deposition

Subrina Rafique,[1,a)] Lu Han,[1,a)] Marko J. Tadjer,[2] Jaime A. Freitas, Jr.,[2] Nadeemullah A. Mahadik,[2] and Hongping Zhao[1,b)]
[1]*Department of Electrical Engineering and Computer Science, Case Western Reserve University, Cleveland, Ohio 44106, USA*
[2]*United States Naval Research Laboratory, Washington, DC 20375, USA*

(Received 1 March 2016; accepted 18 April 2016; published online 5 May 2016)

This paper presents the homoepitaxial growth of phase pure (010) β-Ga_2O_3 thin films on (010) β-Ga_2O_3 substrate by low pressure chemical vapor deposition. The effects of growth temperature on the surface morphology and crystal quality of the thin films were systematically investigated. The thin films were synthesized using high purity metallic gallium (Ga) and oxygen (O_2) as precursors for gallium and oxygen, respectively. The surface morphology and structural properties of the thin films were characterized by atomic force microscopy, X-ray diffraction, and high resolution transmission electron microscopy. Material characterization indicates the growth temperature played an important role in controlling both surface morphology and crystal quality of the β-Ga_2O_3 thin films. The smallest root-mean-square surface roughness of ~7 nm was for thin films grown at a temperature of 950 °C, whereas the highest growth rate (~1.3 μm/h) with a fixed oxygen flow rate was obtained for the epitaxial layers grown at 850 °C. *Published by AIP Publishing.*
[http://dx.doi.org/10.1063/1.4948944]

Ga_2O_3 is a wide bandgap semiconductor material ($E_g \sim 4.9$ eV at room temperature) which exhibits high transparency in the ultraviolet (UV) and visible wavelength regions. Ga_2O_3 is estimated to have a high breakdown field (8 MV/cm) due to its very large bandgap. Among the five known phases (α, β, γ, δ, and ε), β-Ga_2O_3 is most thermodynamically stable. Recently, renewed interest in this material has arisen due to the successful growth of large area, single crystalline β-Ga_2O_3 substrates with excellent structural quality, and controllable doping. These advancements have opened up applications for β-Ga_2O_3 as solar blind photodetectors and high power devices, as well as potential substrates for GaN light emitting diodes. More advantageously, high quality single crystalline β-Ga_2O_3 substrates can be synthesized by melt based methods including the edge-defined film-fed growth (EFG),[1,2] floating zone,[3–8] and Czochralski[9–12] methods. The substrates obtained through these methods are expected to be scalable and low cost.[13]

Recently, β-Ga_2O_3 thin films have been heteroepitaxially grown on foreign substrates such as Al_2O_3, Si, GaAs, ZrO_2:Y, and MgO by molecular beam epitaxy (MBE),[14–16] metal organic chemical vapor deposition (MOCVD),[17–21] mist chemical vapor deposition (CVD),[22] CVD,[23,24] pulsed laser deposition (PLD),[25–27] and radio frequency magnetron sputtering.[28–30] Homoepitaxial growths of β-Ga_2O_3 thin films on (100), (010), and (001) substrates by MBE, MOCVD, and halide vapor phase epitaxy (HVPE) were also reported.[31–37] However, challenges associated with the growth kinetics by conventional epitaxy such as MBE and MOCVD have limited the growth rate ($\ll 1$ μm/h).[38] The fastest growth rate reported to date was ~25 μm/h for the β-Ga_2O_3 homoepitaxial layer on (001) substrate by HVPE.[37] Metal-semiconductor field-effect transistors (MESFETs),[39] metal-oxide-semiconductor FETs (MOSFETs),[40] and Schottky barrier diodes (SBDs)[37] using homoepitaxial β-Ga_2O_3 thin films grown by MBE and HVPE have been demonstrated. Very recently, we reported the heteroepitaxy of β-Ga_2O_3 on sapphire substrate with growth rate of 1.1 μm/h,[24] as well as the synthesis of β-Ga_2O_3 rods on SiC substrate[41] by low pressure chemical vapor deposition (LPCVD).

In this paper, we report the synthesis of single phase β-Ga_2O_3 homoepitaxial layer on (010) β-Ga_2O_3 substrate by LPCVD. The advantages of LPCVD technique include low cost, high reproducibility and scalability, good uniformity of film thickness, and homogeneity of the deposited thin films. The growth of β-Ga_2O_3 homoepitaxial layers on (010) β-Ga_2O_3 substrates were reported previously by ozone MBE and plasma-assisted MBE (PAMBE).[33,34,36] However, the reported growth rate was relatively slow (<0.7 μm/h). For practical high power device applications, film growth with reasonable growth rate and high material quality is crucial. In this paper, we report the homoepitaxial synthesis of β-Ga_2O_3 with a growth rate of ~1.3 μm/h. Growth temperature dependences of surface morphology and crystal quality were investigated.

The homoepitaxial growths of β-Ga_2O_3 thin films were carried out in a custom-designed CVD system. The growth studies reported here were carried out on commercial (010) β-Ga_2O_3 substrates synthesized by the EFG growth method.[1] The dislocation density of the substrate was estimated to be $<10^7$ cm^{-2}. High purity gallium pellets (Alfa Aesar, 99.99999%) and oxygen were used as the source materials and argon (Ar) was used as the carrier gas. To investigate the effect of growth temperature on the crystal quality and surface morphology of the Ga_2O_3 thin films, several experiments were conducted by varying the growth temperature in the range between 780 °C and 950 °C.

[a)]S. Rafique and L. Han contributed equally to this work.
[b)]Author to whom correspondence should be addressed. Electronic mail: hongping.zhao@case.edu.

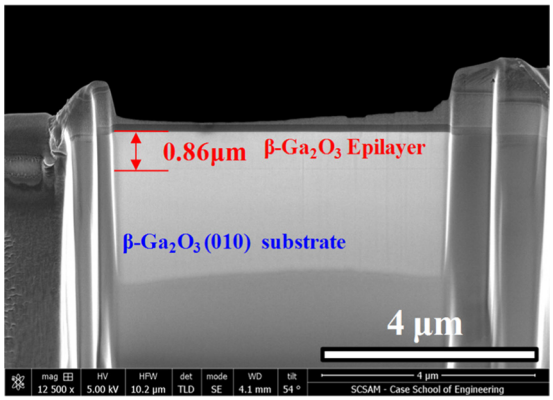

FIG. 1. Cross sectional FESEM image of TEM sample prepared by FIB. The sample was prepared from a β-Ga_2O_3 homoepitaxial layer grown at 850 °C. The β-Ga_2O_3 epi-layer thickness is ~0.86 μm.

The structure, crystal quality, and surface morphology of the β-Ga_2O_3 thin films were characterized by using field emission scanning electron microscopy (FESEM), atomic force microscopy (AFM, Bruker NanoMan), high resolution X-ray diffraction (HR-XRD, Rigaku Smartlab with Cu Kα_1 radiation), transmission electron microscopy (TEM, FEI Tecnai F30), and Raman spectroscopy (laser beam of 532 nm). The cathodoluminescence (CL) spectra were measured in an ultra-high-vacuum chamber, with the electron beam spot size normally is around 100 μm and the energy density is typically kept between 40 and 1000 W/cm^2. To avoid contribution from the substrate to the luminescence spectra of the epitaxial films, the CL measurements of the films were carried out with beam energy of 3 keV, which limits the peak of the rate of energy loss to a depth of less than 50 nm.

Figure 1 shows the cross sectional FESEM image of the β-Ga_2O_3 TEM sample, which was grown at 850 °C for 40 min. From this image, the thickness of the homoepitaxial layer was estimated to be 0.86 μm, which corresponded to a growth rate of ~1.3 μm/h. For comparison, recent reported growth rates for β-Ga_2O_3 homoepitaxial thin films grown on β-Ga_2O_3 substrates were 0.05 μm/h (MBE, (100) native substrate),[32] 0.48 μm/h (MOVPE, (100) native substrate),[35] 0.125 μm/h (MBE, (010) native substrate),[33] 0.7 μm/h (MBE, (010) native substrate),[34] and 5–25 μm/h (HVPE, (001) native substrate),[37] respectively.

To understand the effects of LPCVD growth temperature on the surface morphology of β-Ga_2O_3 homoepitaxial layer, a number of experiments were carried out. Figures 2(a)–2(e) show the AFM images of 5 × 5 μm^2 scan for epitaxial layer surfaces grown at different growth temperatures between 780 and 950 °C. The surface roughness of the epitaxial layer showed a strong dependence on the growth

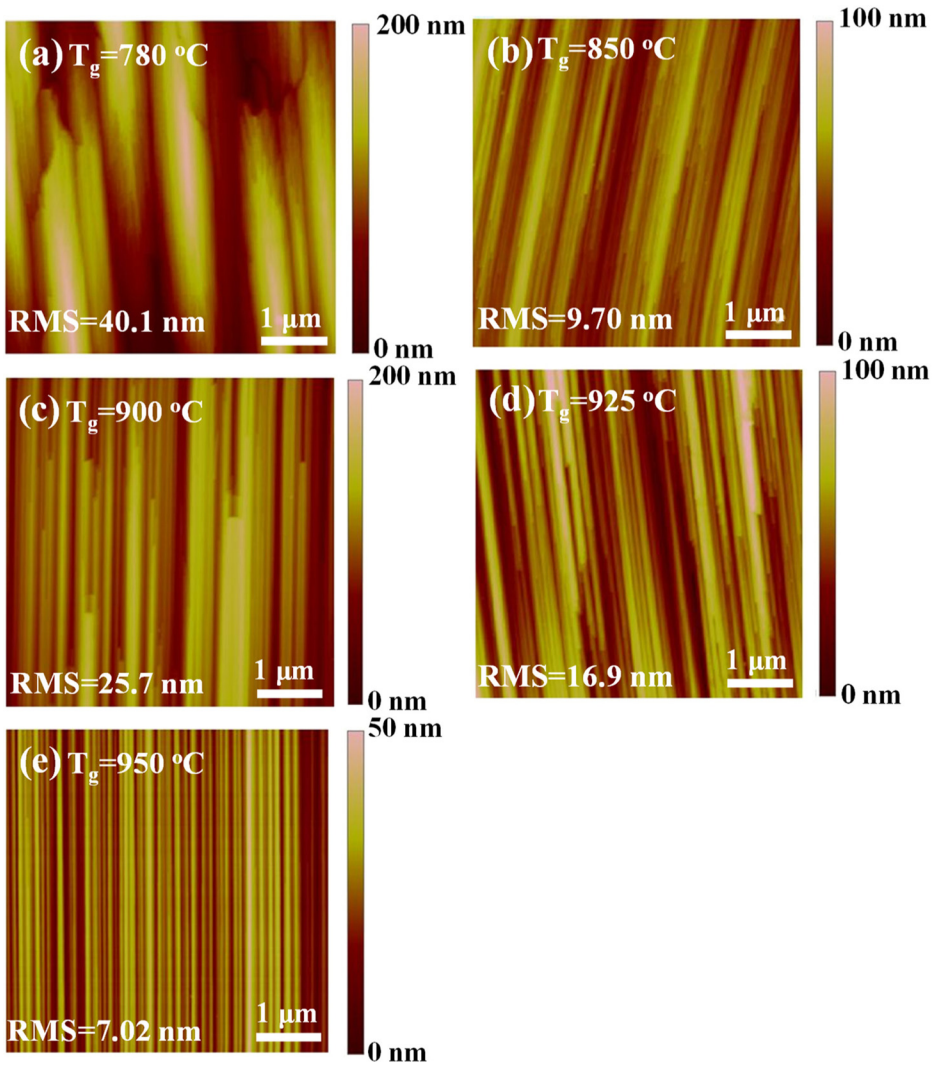

FIG. 2. Surface AFM images (5 μm × 5 μm) of β-Ga_2O_3 homoepitaxial layers grown at different growth temperatures.

temperature. The general trend indicated that the layers became more homogeneous with the increase of growth temperature. All the layers were composed of multi-step arrays resembling terrace-like morphology (similar to that of the substrate). The feature size became smaller with the increase of the growth temperature. The lowest surface RMS roughness was 7.02 nm for the epitaxial layer grown at 950 °C. This may have been due to the reduced film growth rate with the increase of growth temperature as a result of the formation and desorption of Ga_2O.[38] Ga_2O is formed at a higher temperature due to the reaction of excess Ga with Ga_2O_3 surface oxides. Note that precise control of surface roughness is important as it limits the surface roughness dependent component of field effect mobility.

The crystal quality of the β-Ga_2O_3 homoepitaxial layers was characterized by HR-XRD. Figure 3 shows the HR-XRD reflections of the β-Ga_2O_3 (010) substrate and β-Ga_2O_3 homoepitaxial layer grown at 900 °C and 950 °C. Both symmetric and asymmetric (grazing angle) reflections are shown. The high incident angles for the (020) and (-22-1) reflections penetrate all the way through the film and into the substrate for few microns. The (-42-2) reflection was taken at a grazing incidence angle of ~1.5°. Using the dynamical scattering theory, the penetration depth of this reflection was calculated to be ~0.7 μm, indicating most of the signal was from the top film. No peaks associated with other phases (α, γ, δ, and ε) of Ga_2O_3 were detected in the diffraction spectra. This is a good indication that the film has grown homoepitaxially on the substrate and has only β phase. Assuming the β angle to be fixed at 103.83°, the calculated lattice constants for the substrate were: a = 12.1774 Å, b = 3.0373 Å, and c = 5.7968 Å. The grown film was under slight compressive strain evidenced from the shift in the film peak to the left in the Bragg reflection. The calculated compressive strain is 0.11%. For the film grown at 950 °C, a film peak is not observed in the (-42-2) reflection, which may be due to film decomposition at the higher growth temperature.

Figure 4 shows the XRD rocking curves of (-42-2) reflection of β-Ga_2O_3 homoepitaxial layer synthesized at growth temperature of 900 °C and 950 °C. The XRD rocking

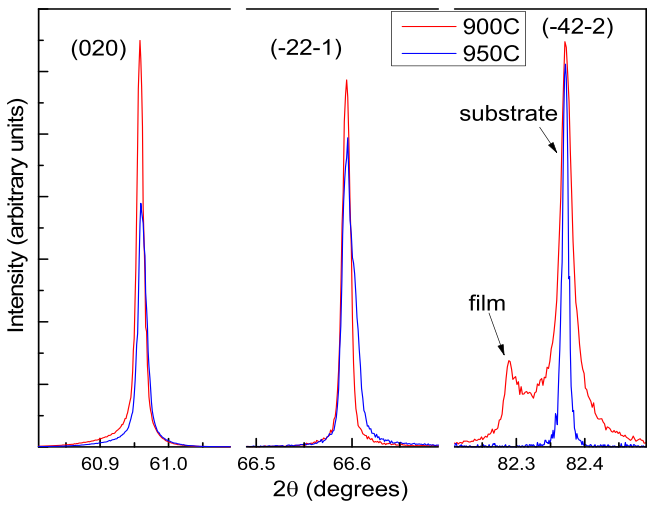

FIG. 3. XRD patterns (2θ scan) of β-Ga_2O_3 (010) substrate and β-Ga_2O_3 homoepitaxial layer grown at 900 °C and 950 °C.

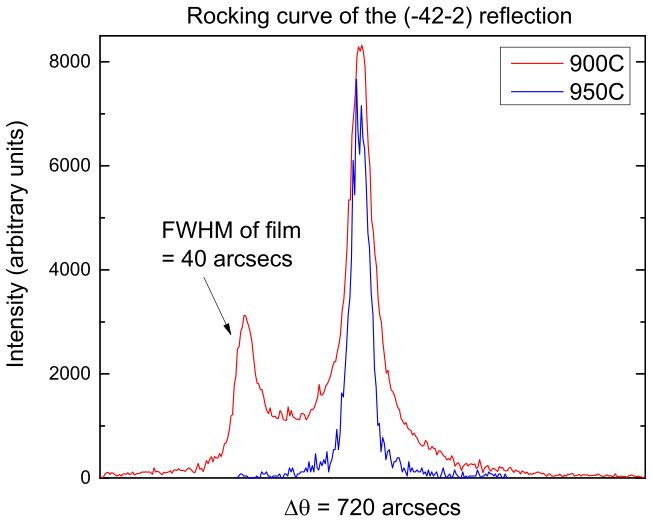

FIG. 4. XRD rocking curves of (-42-2) reflection peak of β-Ga_2O_3 homoepitaxial layer grown at 900 °C and 950 °C.

curve full width at half maximum (FWHM) of (-42-2) peak for the layer grown at 900 °C and the substrate were 40 and ~20 arc sec, respectively. On the film grown at 950 °C, the film peak is not observed and the substrate rocking curve matches the other sample since they are taken from the same substrate material. The recent reported XRD rocking curve FWHMs of β-Ga_2O_3 homoepitaxial layers grown on (100) and (001) β-Ga_2O_3 substrates by MBE and HVPE are 72 (Ref. 32) and 60–78 arc sec,[37] respectively. The reported XRD rocking curve FWHM of these homoepitaxial layers was limited by the quality of their corresponding substrates.[34,37] The small value of the FWHM of the homoepitaxial layer demonstrates a high quality epitaxial film with very low dislocations and strain.

The crystal quality and interfacial structure of the β-Ga_2O_3 homoepitaxial layer grown at 850 °C were further investigated with cross sectional TEM and HRTEM as well as the selected area electron diffraction (SAED) pattern. Figure 5(a) shows the cross sectional TEM image of the homoepitaxial layer. From the HRTEM, the interface between the grown layer and the substrate is undifferentiable along the cross section indicating the layer is epitaxially grown on the substrate. Figure 5(b) shows the SAED pattern of the layer taken along the [-20-1] zone axis. The SAED pattern confirms that the synthesized thin film is single crystalline monoclinic β-Ga_2O_3. The lattice-resolved HRTEM image of the homoepitaxial layer is shown in Fig. 5(c). The lattice planes were well aligned along the growth direction. From the HRTEM image of Fig. 5(c), the lattice fringes with marked interplanar distances of 0.15 nm and 0.21 nm, which correspond to d-spacings of monoclinic β-Ga_2O_3 (020) and (-112) planes, respectively.[42]

Room temperature Raman spectra of the β-Ga_2O_3 (010) substrate and a homoepitaxial layer grown at 850 °C are shown in Fig. 6. β-Ga_2O_3 has a monoclinic structure and belongs to the C_{2h} space group.[43–46] The low frequency modes 168.98 and 199.83 cm^{-1} are attributed to the vibration and translation of tetrahedra-octahedra chains. The mid frequency modes 320.21, 346.77, 416.60, and 480.86 cm^{-1} are related to the deformation of Ga_2O_6 octahedra. The high

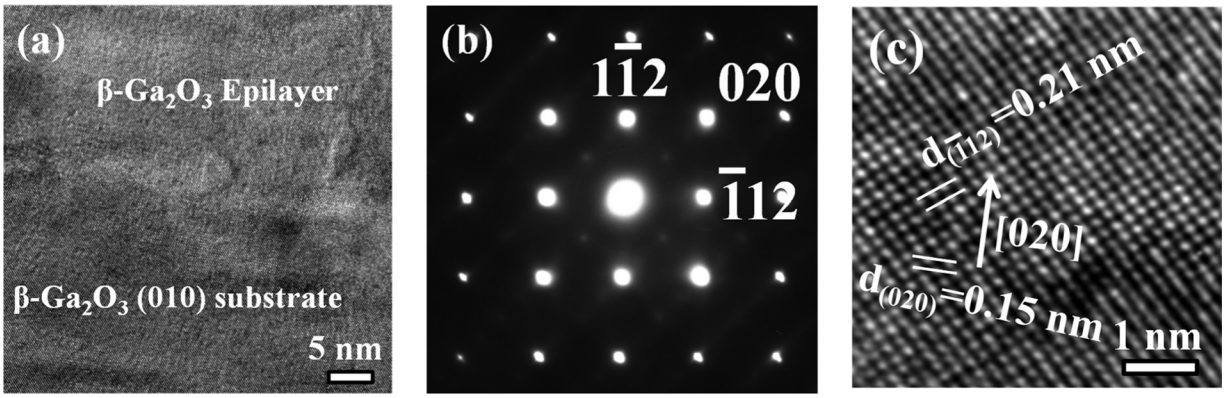

FIG. 5. (a) Cross sectional TEM image of β-Ga_2O_3 homoepitaxial layer grown on β-Ga_2O_3 (010) substrate at 850 °C. (b) SAED pattern of β-Ga_2O_3 homoepitaxial layer taken along [-20-1] zone axis. (c) HRTEM image of β-Ga_2O_3 homoepitaxial layer showing the lattice fringes.

frequency modes 629.94, 658.21, and 766.17 cm^{-1} represent the bending and stretching of GaO_4 tetrahedra. By comparing the Raman spectrum of the grown film with that of the substrate, the low frequency Raman modes are more prominent in intensities than the remaining modes in mid and high frequency modes. A negligible shift of the Raman peak positions for the epitaxial layer comparing to those of the substrate is within the measurement tolerance limit. Thus, the grown epitaxial layer is under no significant strain which corroborates our conclusion from the XRD measurements. Only allowed β-Ga_2O_3 modes are observed in the Raman spectra indicating the absence of other Ga_2O_3 phases. These results suggest that the as-synthesized β-Ga_2O_3 homoepitaxial layer is phase pure and of high crystal quality.

The room temperature CL spectra of the β-Ga_2O_3 homoepitaxial layers grown at 900 °C and 950 °C are shown in Fig. 7. The peak near ~4.9 eV corresponding to band to band recombination is absent for both samples. The CL intensity for the homoepitaxial film grown at 950 °C is higher than that of the film grown at 900 °C, suggesting that the thin film grown at 950 °C has lower concentration of non-radiative recombination centers and thus indicating improved optical quality. The relatively broadbands in the blue-UV emission range (2.9–3.5 eV) are attributed to the self-trapped excitons and donor–acceptor pair transitions. Oxygen vacancies (V_O) or Ga interstitials introduced the donor levels and $V_O - V_{Ga}$ pairs acted as the acceptor centers.[47] Further optimization of the growth conditions is still required to advance the material quality with controllable electrical transport properties aiming device applications. Recently, we demonstrated the effective n-type doping in β-Ga_2O_3 thin films grown by LPCVD. The details of the doping procedure and material properties will be reported in a future publication.

In summary, we have demonstrated the synthesis of homoepitaxial β-Ga_2O_3 layer with high purity and high structural quality on β-Ga_2O_3 (010) substrate by LPCVD. Our studies show that the growth temperature is a crucial parameter for controlling the growth of β-Ga_2O_3 thin films by LPCVD. We obtained β-Ga_2O_3 homoepitaxial thin films with RMS surface roughness of ~7 nm and growth rate of ~1.3 μm/h for the thin films grown at 950 °C and 850 °C, respectively. The demonstration of the homoepitaxy of β-Ga_2O_3 thin films with high material quality and reasonable

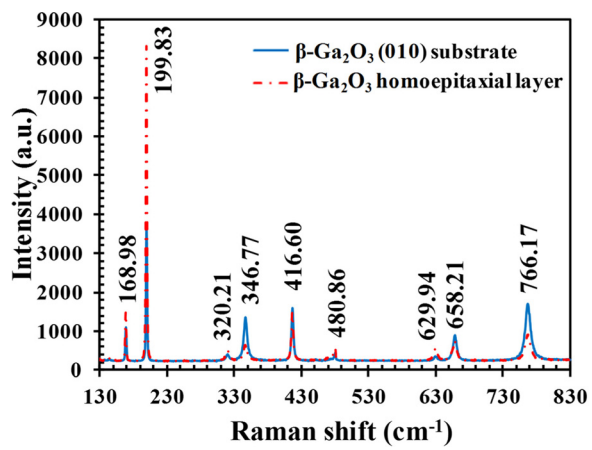

FIG. 6. Micro-Raman spectra of β-Ga_2O_3 (010) substrate and β-Ga_2O_3 homoepitaxial layer grown at 850 °C.

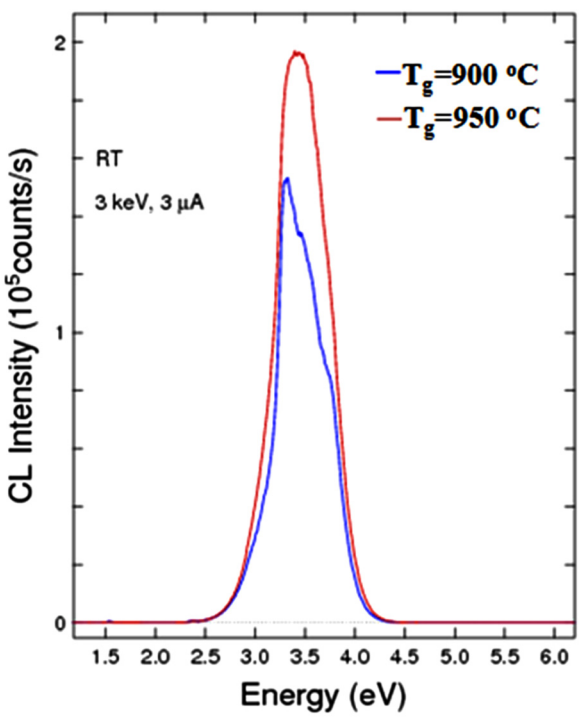

FIG. 7. Room temperature CL spectra of β-Ga_2O_3 homoepitaxial layers grown at 900 °C and 950 °C.

growth rate is important for β-Ga_2O_3 as a potential candidate for future device applications in high power devices and solar blind photodetectors.

Part of the material characterization was performed at the Swagelok Center for Surface Analysis of Materials (SCSAM) at CWRU, and at the Lurie Nanofabrication Facility (LNF) at the University of Michigan. The Raman spectra measurements were performed at Dr. Philip Feng's Laboratory at CWRU. Research at NRL was supported by the Office of Naval Research.

[1]H. Aida, K. Nishiguchi, H. Takeda, N. Aota, K. Sunakawa, and Y. Yaguchi, Jpn. J. Appl. Phys., Part 1 **47**, 8506 (2008).
[2]T. Oishi, Y. Koga, K. Harada, and M. Kasu, Appl. Phys. Express **8**, 031101 (2015).
[3]Y. Tomm, J. M. Ko, A. Yoshikawa, and T. Fukuda, Sol. Energy Mater. Sol. Cells **66**, 369 (2001).
[4]E. G. Villora, K. Shimamura, Y. Yoshikawa, K. Aoki, and N. Ichinose, J. Cryst. Growth **270**, 420 (2004).
[5]J. Zhang, B. Li, C. Xia, G. Pei, Q. Deng, Z. Yang, W. Xu, H. Shi, F. Wu, Y. Wu, and J. Xu, J. Phys. Chem. Solids **67**, 2448 (2006).
[6]S. Ohira, N. Suzuki, N. Arai, M. Tanaka, T. Sugawara, K. Nakajima, and T. Shishido, Thin Solid Films **516**, 5763 (2008).
[7]E. G. Villora, K. Shimamura, Y. Yoshikawa, T. Ujiie, and K. Aoki, Appl. Phys. Lett. **92**, 202120 (2008).
[8]T. C. Lovejoy, E. N. Yitamben, N. Shamir, J. Morales, E. G. Villora, K. Shimamura, S. Zheng, F. S. Ohuchi, and M. A. Olmstead, Appl. Phys. Lett. **94**, 081906 (2009).
[9]Z. Galazka, R. Uecker, K. Irmscher, M. Albrecht, D. Klimm, M. Pietsch, M. Brutzam, R. Bertram, S. Ganschow, and R. Fornari, Cryst. Res. Technol. **45**, 1229 (2010).
[10]K. Irmscher, Z. Galazka, M. Pietsch, R. Uecker, and R. Fornari, J. Appl. Phys. **110**, 063720 (2011).
[11]Z. Galazka, K. Irmscher, R. Uecker, M. Albrecht, R. Bertram, M. Pietsch, A. Kwasneiwski, M. Naumann, T. Schulaz, R. Schewski, D. Klimm, and M. Bickermann, J. Cryst. Growth **404**, 184 (2014).
[12]M. Handwerg, R. Mitdank, Z. Galazka, and S. F. Fischer, Semicond. Sci. Technol. **30**, 024006 (2015).
[13]M. Higashiwaki, K. Sasaki, A. Kuramata, T. Masui, and S. Yamakoshi, Phys. Status Solidi A **211**, 21 (2014).
[14]T. Oshima, T. Okuno, and S. Fujita, Jpn. J. Appl. Phys., Part 1 **46**, 7217 (2007).
[15]D. Guo, Z. Wu, P. Li, Y. An, H. Liu, X. Guo, H. Yan, G. Wang, C. Sun, L. Li, and W. Tang, Opt. Mater. Express **4**, 1067 (2014).
[16]X. Z. Liu, P. Guo, T. Sheng, L. X. Qian, W. L. Zhang, and Y. R. Li, Opt. Mater. **51**, 203 (2016).
[17]V. Gottschalch, K. Mergenthaler, G. Wagner, J. Bauer, H. Paetzelt, C. Sturm, and U. Teschner, Phys. Status Solidi A **206**, 243 (2009).
[18]Y. Lv, J. Ma, W. Mi, C. Luan, Z. Zhu, and H. Xiao, Vacuum **86**, 1850 (2012).
[19]W. Mi, J. Ma, Z. Zhu, C. Luan, Y. Lv, and H. Xiao, J. Cryst. Growth **354**, 93 (2012).
[20]N. M. Sbrockey, T. Salagaj, E. Coleman, G. S. Tompa, Y. Moon, and M. S. Kim, J. Electron. Mater. **44**, 1357 (2015).
[21]M. J. Tadjer, M. A. Mastro, N. A. Mahadik, M. Currie, V. D. Wheeler, J. A. Freitas, Jr., J. D. Greenlee, J. K. Hite, K. D. Hobart, C. R. Eddy, Jr., and F. J. Kub, J. Electron. Mater. **45**, 2031 (2016).
[22]K. Kaneko, H. Ito, S.-D. Lee, and S. Fujita, Phys. Status Solidi C **10**, 1596 (2013).
[23]T. Terasako, H. Ichinotani, and M. Yagi, Phys. Status Solidi C **12**, 985 (2015).
[24]S. Rafique, L. Han, and H. Zhao, Phys. Status Solidi A **213**, 1002 (2016).
[25]S.-L. Ou, D.-S. Wuu, Y.-C. Fu, S.-P. Liu, R.-H. Horng, L. Liu, and Z.-C. Feng, Mater. Chem. Phys. **133**, 700 (2012).
[26]S. Muller, H. V. Wenckstern, D. Splith, F. Schmidt, and M. Grundmann, Phys. Status Solidi A **211**, 34 (2014).
[27]F. B. Zhang, K. Saito, T. Tanaka, M. Nishio, and Q. X. Guo, J. Cryst. Growth **387**, 96 (2014).
[28]Y. Wei, Y. Jinliang, W. Jiangyan, and Z. Liying, J. Semicond. **33**, 073003 (2012).
[29]K. H. Choi and H. C. Kang, Mater. Lett. **123**, 160 (2014).
[30]Z. Wu, G. Bai, Q. Hu, D. Guo, C. Sun, L. Ji, M. Lei, L. Li, P. Li, J. Hao, and W. Tang, Appl. Phys. Lett. **106**, 171910 (2015).
[31]T. Oshima, N. Arai, N. Suzuki, S. Ohira, and S. Fujita, Thin Solid Films **516**, 5768 (2008).
[32]M.-Y. Tsai, O. Bierwagen, M. E. White, and J. S. Speck, J. Vac. Sci. Technol., A **28**, 354 (2010).
[33]K. Sasaki, A. Kuramata, T. Masui, E. G. Villora, K. Shimamura, and S. Yamakoshi, Appl. Phys. Express **5**, 035502 (2012).
[34]K. Sasaki, M. Higashiwaki, A. Kuramata, T. Masui, and S. Yamakoshi, J. Cryst. Growth **392**, 30 (2014).
[35]G. Wagner, M. Baldini, D. Gogova, M. Schmidbauer, R. Schewski, M. Albrecht, Z. Galazka, D. Klimm, and R. Fornari, Phys. Status Solidi A **211**, 27 (2014).
[36]H. Okumura, M. Kita, K. Sasaki, A. Kuramata, M. Higashiwaki, and J. S. Speck, Appl. Phys. Express **7**, 095501 (2014).
[37]H. Murakami, K. Nomura, K. Goto, K. Sasaki, K. Kawara, Q. T. Thieu, R. Togashi, Y. Kumagai, M. Higashiwaki, A. Kuramata, S. Yamakoshi, B. Monemar, and A. Koukitu, Appl. Phys. Express **8**, 015503 (2015).
[38]P. Vogt and O. Bierwagen, Appl. Phys. Lett. **108**, 072101 (2016).
[39]M. Higashiwaki, K. Sasaki, A. Kuramata, T. Masui, and S. Yamakoshi, Appl. Phys. Lett. **100**, 013504 (2012).
[40]M. Higashiwaki, K. Sasaki, T. Kamimura, M. H. Wong, D. Krishnamurthy, A. Kuramata, T. Masui, and S. Yamakoshi, Appl. Phys. Lett. **103**, 123511 (2013).
[41]S. Rafique, L. Han, C. A. Zorman, and H. Zhao, Cryst. Growth Des. **16**, 511 (2016).
[42]H.-S. Chung, S. C. Kim, D. H. Kim, J. W. Kim, O.-J. Kwon, C. Park, and K. H. Oh, J. Korean Phys. Soc. **55**, 68 (2009).
[43]X. Du, W. Mi, C. Luan, Z. Li, C. Xia, and J. Ma, J. Cryst. Growth **404**, 75 (2014).
[44]X. Du, Z. Li, C. Luan, W. Wang, M. Wang, X. Feng, H. Xiao, and J. Ma, J. Mater. Sci. **50**, 3252 (2015).
[45]D. Gogova, M. Schmidbauer, and A. Kwasniewski, Cryst. Eng. Commun. **17**, 6744 (2015).
[46]S. Kumar, G. Sarau, C. Tessarek, M. Y. Bashouti, A. Hahnel, S. Christiansen, and R. Singh, J. Phys. D: Appl. Phys. **47**, 435101 (2014).
[47]J. Diaz, I. Lopez, E. Nogales, B. Mendez, and J. Piqueras, J. Nanopart. Res. **13**, 1833 (2011).